On the Dynamics of Wind-Driven Lake Currents

JOHN R. BENNETT

IFYGL Project Office, NOAA, Rockville, Md. 20852

(Manuscript received 19 July 1973, in revised form 8 January 1974)

ABSTRACT

Two time-dependent "vertical cross section models" are analyzed and applied to wind-driven currents in Lake Ontario. The models are: 1) a linear frictionless, two-level model, and 2) a numerical model which includes both friction and nonlinear terms. They predict current and temperature under the assumption that all variables except pressure are independent of the longshore coordinate. The longshore pressure gradient is computed from the condition that the volume transport normal to the cross section is zero.

First, the quasi-static response of the linear frictionless model is studied to isolate the effects of topography and stratification on the structure of the coastal currents. It predicts that the vertically averaged longshore current is independent of both rotation and stratification, being in the direction of the wind where the water is shallower than average and opposite the wind in the deep water. Under homogeneous conditions, the strongest currents are confined to a thin (~3 km wide for Lake Ontario) region near the shore. The effect of stratification is to increase the width of this "coastal jet" region and cause the flow to be more confined to the surface layer.

These qualitative results of the linear model are also true for the numerical model, but the latter gives more realistic current magnitudes. The main differences between the two models are due to friction which has a relatively straightforward damping effect on both the quasi-geostrophic and inertial oscillation components of the flow. The damping of the geostrophic mode, however, is smaller in cases where stratification is important, because it decreases the effect of bottom friction.

The models give realistic magnitudes for both horizontal and vertical motion in Lake Ontario and can explain many of the differences between the spring and summer current regimes.

1. Introduction

This paper presents a time-dependent theory of wind-generated currents and upwelling in the Great Lakes. Many of the calculations are done with parameters appropriate to Lake Ontario since it is one of the most studied lakes and a large field program—The International Field Year for the Great Lakes—is currently being conducted on it. However, the basic physics applies equally well to the other lakes as well as to the continental shelf regions of the oceans.

Typical of the observations which motivate this work are those of Csanady (1972b, c). He found that the currents in the region within 15 km of the north shore of Lake Ontario differ markedly from those in the central region of the lake. In the interior the flow is typically about 5 cm sec^{-1}, and shows no preference in direction; quite often inertial oscillations predominate. In the shore region, however, the flow is mainly longshore and of higher velocity. He suggested that stratification, inertial accelerations, bottom topography and friction may all be important in the boundary region.

For several years similar coastal currents on the south shore of Lake Ontario have been studied by J. T. Scott and his associates (Scott and Lansing, 1967; Scott and Landsberg, 1969; Landsberg *et al.*, 1970; Scott *et al.*, 1971). In addition, they attempted to relate their observations to the lakewide circulation rather than just to the local region they studied. They speculated that the transport of water was in the same direction on both sides of the lake, with a return flow in the central region.

In general, these studies have not shown any obvious correlation between the wind and the simultaneous current. Most of the observers believe the time history of the wind is at least as important as the instantaneous value. However, most of the existing theories either assume steady-state flow in which frictional dissipation balances wind forcing or include time-dependence but not friction.

The steady-state theories have largely been confined to studying the linearized, vertically integrated equations for flow in a homogeneous lake. Using this approach, Birchfield (1967a) studied a circular lake of parabolic depth profile and Rao and Murty (1970) studied circulation patterns in Lake Ontario. The main weakness of this type of theory is that it only predicts values of the depth average of the current. Birchfield (1972, 1973) has attempted to remedy this

weakness and to generalize his theory to basins of arbitrary shape and topography.

Much of the inviscid time-dependent theory is due to G. T. Csanady who was influenced by earlier work on geostrophic adjustment by Rossby (1938) and Charney (1955). In a series of papers (1967, 1968a, b), he studied the response of a two-layer lake of constant depth to a uniform wind stress. Some of his results were later corrected by Birchfield (1969). Csanady expanded this theory to include the effect of continuous stratification (1972a). In all these problems the response of the model lake is the sum of external and internal inertio-gravity waves and a quasi-static response in which the current is largest near the shore and the longshore component is geostrophic. The quasi-static response can be computed relatively easily for models which include both stratification and topography. This is done in Section 2.

The recent theory of Walin (1972) is related to both Csanady's and Birchfield's. It is essentially an inviscid time-dependent theory as is Csanady's. However, like Birchfield, Walin believes that far enough away from the side walls the flow is strongly controlled by topography. Both deduce that the Taylor-Proudman constraint applys, i.e., the geostrophic component of the flow follows the bottom contours.

Most of the theories which include both friction and time dependence are numerical models which are applied to realistic basins; the authors have not attempted to generalize their results. The models most relevant to this study are those of Paskausky (1971) and Simons (1971a, b, 1972) since they studied Lake Ontario. Paskausky's model is a vertically integrated model which neglects stratification. Simons' model is three dimensional and includes stratification.

The goal of this study is not to duplicate these modeling efforts for Lake Ontario but to discuss the dynamics of the currents. This, hopefully, will allow one to draw some general conclusions about the wind-driven circulation in other lakes where topography and stratification differ from that of Lake Ontario.

Some of the questions we wish to answer are:

1. What general pattern of large-scale currents would be generated if a storm passes over a lake?
2. What is the relative importance of topography, rotation, friction, inertial accelerations and stratification in determining the currents?

These questions can best be answered by using simplified models, each of which isolates only a few of the physical processes. Thus, an earlier study (Bennett, 1972) uses a model which included stratification, longshore propagation of baroclinic Kelvin waves, and nonlinear effects, but not topography and friction. In the present study, longshore propagation and advection are excluded. The models used here predict the flow in a vertical cross section under the assumption that current and temperature are independent of the longshore direction.

The equations for these "cross-section models" differ from those for an infinite channel only in that a longshore ("setup") pressure gradient is allowed so that the total volume transport normal to the cross section is zero. In order for this longshore pressure gradient to be consistent with the assumption that velocity and temperature are independent of the longshore coordinate, it must be a function only of time. This variation of the infinite channel model was used by Birchfield (1967b) and has recently been employed in numerical studies by Hurlburt and Thompson (1972) and Killworth (1973). Both of these latter two first studied models which neglected the longshore pressure gradient (O'Brien and Hurlburt, 1972). The physical justification for this approximation is that the longshore pressure gradient becomes established in a fraction of the external seiche period of the lake, but internal waves and low-frequency quasi-geostrophic motions respond to the end walls on a much longer time scale. The oscillatory component of the surface pressure gradient, the seiche, has the same magnitude as the setup component (Rao, 1967), but, since it has a shorter time scale, generates weaker currents. It is not surprising, therefore, that the three-dimensional, time-dependent model of Simons (1971a, 1972) predicts flow patterns with very little longshore variation in the central region of Lake Ontario, and which, to a good approximation, obey the constraint that the volume transport normal to the cross section is zero.

One of the cross-section models used here is linearized and frictionless. The other is a numerical model which is used to evaluate the effects of bottom friction and the nonlinear inertial terms. Both assume the validity of the hydrostatic, Boussinesq and rigid lid approximations. The first two are standard in oceanography and will not be discussed here. The third is common but requires justification.

In the rigid lid approximation, displacements of the free surface are neglected in the equation of continuity. The equations are then the same as those describing the motion of a fluid in a basin with a rigid lid. The pressure under the lid can be related hydrostatically to the free surface displacement in a real lake. The major consequence of this approximation is that surface gravity waves are filtered out. There is a negligible effect on low-frequency topographic waves as long as the quantity

$$\epsilon=\frac{L^2f^2}{gH}$$

is small (Ball, 1965). Here, L is a typical horizontal length, f the Coriolis parameter, g gravity and H a typical depth. This ratio is the square of the ratio of the fundamental seiche period to the inertial period. In Lake Ontario the seiche period is about 5 hr and

the inertial period is about 16 hr. Thus, $\epsilon \approx 0.1$, and it is reasonable to neglect this effect. A more thorough analysis of the rigid lid approximation in lake models is currently being made by Lick (1972).

In Section 2 the quasi-static response of the linear frictionless model is studied in an attempt to isolate the influence of topography and stratification on the structure of the coastal currents. This discussion prepares the way for the numerical model of Section 3 which evaluates the effects of friction and nonlinearity. Finally in Section 4 the results of these models are summarized and compared with the Lake Ontario observations.

2. A linear frictionless model

a. The general problem

In this section an attempt is made to isolate the effects of topography and stratification on the structure of the coastal currents. To do this, in addition to the assumptions discussed in Section 1, the following simplifications are made:

1. The lake is composed of two layers of fluid of different density.
2. All nonlinear terms are negligible.
3. Both the interfacial stress between the layers and the bottom stress are zero. Thus, friction plays no role in determining the average current in each layer.
4. The motion is driven by a horizontally uniform surface wind stress.

The pressure just under the rigid lid is denoted as $\rho_0 g\eta$ to emphasize that in a lake this pressure corresponds to a free-surface displacement of η. The other variables are as follows:

x	coordinate normal to shore
y	longshore coordinate
z	vertical coordinate
t	time
$u(x,z,t)$	x component of velocity
$v(x,z,t)$	y component of velocity
$\xi(x,t)$	thermocline displacement
h_1	initial depth of upper layer (constant)
$h_2(x)$	initial depth of lower layer (variable)
L_x	width of lake
$\bar{H}$	average depth $\left[\equiv \frac{1}{L_x}\int_0^{L_x}(h_1+h_2)dx\right]$
τ_x	x component of surface stress
τ_y	y component of surface stress
ρ_0	density of the lower layer
$\Delta\rho$	density difference between the layers
f	the Coriolis parameter (10^{-4} sec^{-1})
g	the gravitational acceleration (980 cm sec^{-2})

The vertically integrated equations of motion and continuity are as follows:

$$\frac{\partial U_1}{\partial t} - fV_1 = -gh_1\frac{\partial \eta}{\partial x} + \frac{\tau_x}{\rho_0} \tag{2.1}$$

$$\frac{\partial V_1}{\partial t} + fU_1 = -gh_1\frac{\partial \eta}{\partial y} + \frac{\tau_y}{\rho_0} \tag{2.2}$$

$$\frac{\partial \xi}{\partial t} - \frac{\partial U_1}{\partial x} = 0 \tag{2.3}$$

$$\frac{\partial U_2}{\partial t} - fV_2 = -gh_2(x)\frac{\partial \eta}{\partial x} - g\frac{\Delta\rho}{\rho_0}h_2(x)\frac{\partial \xi}{\partial x} \tag{2.4}$$

$$\frac{\partial V_2}{\partial t} + fU_2 = -gh_2(x)\frac{\partial \eta}{\partial y} \tag{2.5}$$

$$\frac{\partial \xi}{\partial t} + \frac{\partial U_2}{\partial x} = 0. \tag{2.6}$$

The volume transports are defined by

$$\left.\begin{aligned} U_1 &= \int_{-h_1}^{0} u\,dz, \qquad V_1 = \int_{-h_1}^{0} v\,dz \\ U_2 &= \int_{-(h_1+h_1)}^{-h_1} u\,dz, \quad V_2 = \int_{-(h_1+h_1)}^{-h_1} v\,dz \end{aligned}\right\}.$$

Without the Boussinesq approximation, there would be an additional term $[(\Delta\rho/\rho_0)h_2(x)(\partial\eta/\partial x)]$ on the right-hand side of (2.4) and a similar term in (2.5). If the rigid lid approximation is not made, there would be a term $-\partial\eta/\partial t$ on the left-hand side of (2.3).

The longshore pressure gradient term must be the same in both layers since the density is assumed to be independent of y. It must also be independent of x since otherwise (2.1) would imply that either V_1 or U_1 would be a function of y. The magnitude of this pressure gradient can be determined by adding (2.2) and (2.5) to give

$$\frac{\partial}{\partial t}(V_1+V_2) + f(U_1+U_2) = -g(h_1+h_2)\frac{\partial \eta}{\partial y} + \frac{\tau_y}{\rho_0}. \tag{2.7}$$

From (2.3) and (2.6) and the boundary conditions that $U_1=U_2=0$ at $x=0$, it follows that $U_1+U_2=0$. If (2.7) is integrated from one shore to the other ($x=0$ to $x=L_x$) and we impose the assumption that

$$\int_0^{L_x}(V_1+V_2)dx = 0,$$

then

$$g\frac{\partial \eta}{\partial y} = \frac{\tau_y}{\rho_0\bar{H}}, \tag{2.8}$$

where

$$\bar{H}=(1/L_x)\int_0^{L_x}(h_1+h_2)dx$$

is the average depth.

The condition that the volume transport normal to the cross section is zero, discussed in more detail in Section 1, is imposed because the Great Lakes are nearly closed basins. It would be exactly true for a three-dimensional rigid lid model.

Eq. (2.8) is the classical relation for wind "setup." It is well known that water level fluctuations in lakes can be accounted for reasonably well by using this formula and an empirical relation between the wind speed and surface stress (Platzman, 1963). The time for the mass adjustment to occur is a fraction of the fundamental seiche period. For Lake Ontario this would be a few hours. With the rigid lid approximation the model lake responds instantaneously.

In the general initial value problem discussed here, the lake is assumed to be at rest and the wind stress is zero at $t=0$. At this time the wind stress is suddenly imposed and remains constant thereafter. The initial and boundary conditions are thus:

$$\left.\begin{aligned} t=0:&\quad U_1=U_2=V_1=V_2=0,\quad \xi=\eta=0\\ x=0,L_x:&\quad U_1=U_2=0\end{aligned}\right\}. \tag{2.9}$$

b. Separation of the general problem

Since the equations are linear, the response to the x and y components of the wind can be added to give the response to a wind of arbitrary direction. The response to one component of the wind stress can be obtained by setting the other component equal to zero and solving (2.1)–(2.6) subject to conditions (2.8) and (2.9).

The response to the longshore (y) component of the wind will be further split into a quasi-static response, growing linearly with time, and an oscillatory response. The quasi-static component of the flow is called quasi-geostrophic by Charney (1955). In the terminology of Hess (1959), it is the sum of the purely geostrophic flow and the isallobaric flow. The quasi-static response is of the form

$$\left.\begin{aligned} V_1&=tV_1'(x)\\ V_2&=tV_2'(x)\\ \xi&=t\xi'(x)\\ \frac{\partial\eta}{\partial x}&=t\frac{\partial\eta'}{\partial x}\\ U_1&=U_1'(x)\\ U_2&=U_2'(x)\end{aligned}\right\}. \tag{2.10}$$

The primed variables will be chosen so that the quasi-static response satisfies Eqs. (2.1)–(2.6) and all the auxiliary conditions except the condition $U_1=U_2=0$ at $t=0$. To complete the solution, one must add a solution of the equations with τ_y set to zero, which cancels the quasi-static response at $t=0$. This part of the solution is not very different from the sum of near-inertial-frequency internal waves discussed by Csanady (1968a, b) and Birchfield (1969), and will not be discussed here.

To compute the quasi-static response, we insert (2.8) and (2.10) into (2.1)–(2.6) to obtain

$$fV_1'=gh_1\frac{\partial\eta'}{\partial x} \tag{2.11}$$

$$V_1'+fU_1'=\frac{\tau_y}{\rho_0}\left(1-\frac{h_1}{\bar{H}}\right) \tag{2.12}$$

$$\xi'=\frac{\partial U_1'}{\partial x} \tag{2.13}$$

$$fV_2'=gh_2\frac{\partial\eta'}{\partial x}+g\frac{\Delta\rho}{\rho_0}h_2\frac{\partial\xi'}{\partial x} \tag{2.14}$$

$$V_2'+fU_2'=-\frac{h_2}{\bar{H}}\frac{\tau_y}{\rho_0} \tag{2.15}$$

$$\xi'+\frac{\partial U_2'}{\partial x}=0. \tag{2.16}$$

If one now uses (2.11) and (2.14) to eliminate V_1' and V_2' and then eliminates $\partial\eta'/\partial x$ and U_1', the problem reduces to

$$\left[\frac{g\frac{\Delta\rho}{\rho_0}h_1h_2}{f^2(h_1+h_2)}\right]\frac{\partial\xi'}{\partial x}+U_2'=-\frac{\tau_y}{f\rho_0}\left(\frac{h_2}{h_1+h_2}\right), \tag{2.17}$$

$$\xi'+\frac{\partial U_2'}{\partial x}=0, \tag{2.18}$$

$$U_2'=0 \text{ at } x=0, L_x. \tag{2.19}$$

The other transports can be calculated from

$$U_1'=-U_2',$$

$$V_1'=\frac{\tau_y}{\rho_0}\left(1-\frac{h_1}{\bar{H}}\right)+fU_2',$$

$$V_2'=-\frac{h_2}{\bar{H}}\frac{\tau_y}{\rho_0}-fU_2'.$$

Note that

$$V_1'+V_2'=\frac{\tau_y}{\rho_0}\left(1-\frac{h_1+h_2}{\bar{H}}\right).$$

In other words, the total transport field can be determined immediately. It is independent of the density difference between the layers and of the Coriolis parameter. This flow is in the direction of the wind where the water is shallower than $\bar{H}$ and opposite the wind where the lake is deeper than average; it is zero if the bottom is flat.

c. The quasi-static response to a longshore wind: $\Delta\rho=0$

For the special case of zero density difference between the layers, the solution of (2.17)–(2.18) is

$$\left.\begin{aligned} U_2' &= -\frac{\tau_y}{\rho_0 f}\left(\frac{h_2}{h_1+h_2}\right) \\ \xi' &= \frac{\tau_y}{\rho_0}\frac{\partial}{\partial x}\left(\frac{h_2}{h_1+h_2}\right) \\ V_1' &= \frac{\tau_y}{\rho_0}\left(1-\frac{h_1}{\bar{H}}-\frac{h_2}{h_1+h_2}\right) \\ V_2' &= \frac{\tau_y}{\rho_0}\left(\frac{h_2}{h_1+h_2}-\frac{h_2}{\bar{H}}\right) \end{aligned}\right\}. \qquad (2.20)$$

There are several consequences of taking this limit. First, one cannot satisfy the boundary condition $U_1'=U_2'=0$ at the shore unless $h_2=0$ there; even then it is not a meaningful condition since the division between the two layers is arbitrary. Thus, the solution is only reasonable if it is interpreted as the "interior flow" and one relies on frictional regions near the coast to bring the normal flow to zero. Second, the average longshore current in each layer is the same. Third, ξ must be interpreted as the vertical displacement of the water originally at a depth of h_1, not as the thermocline depth.

The easiest way to interpret these solutions is to plot the average current in each layer after a given wind has been blowing a given amount of time. If the wind stress is 1 dyn cm^{-2} toward the positive y direction and it lasts 10^5 sec (1.1 day), the longshore current and "thermocline" displacement for the quasi-static response are given in Fig. 2a for the lake cross section, similar to that of Lake Ontario, shown in Fig. 1. In this cross section, the depth at the shore has arbitrarily been set equal to 20 m.

The two most significant features of the solution are the thin (3 km e-folding width) coastal current and upwelling regions. The longshore current is barotropic and has a maximum value of about 40 cm sec^{-1}. The

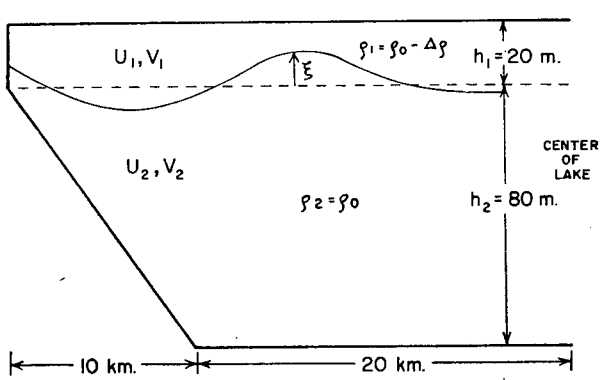

FIG. 1. Idealized cross section of Lake Ontario with definition of variables used in the linear frictionless model.

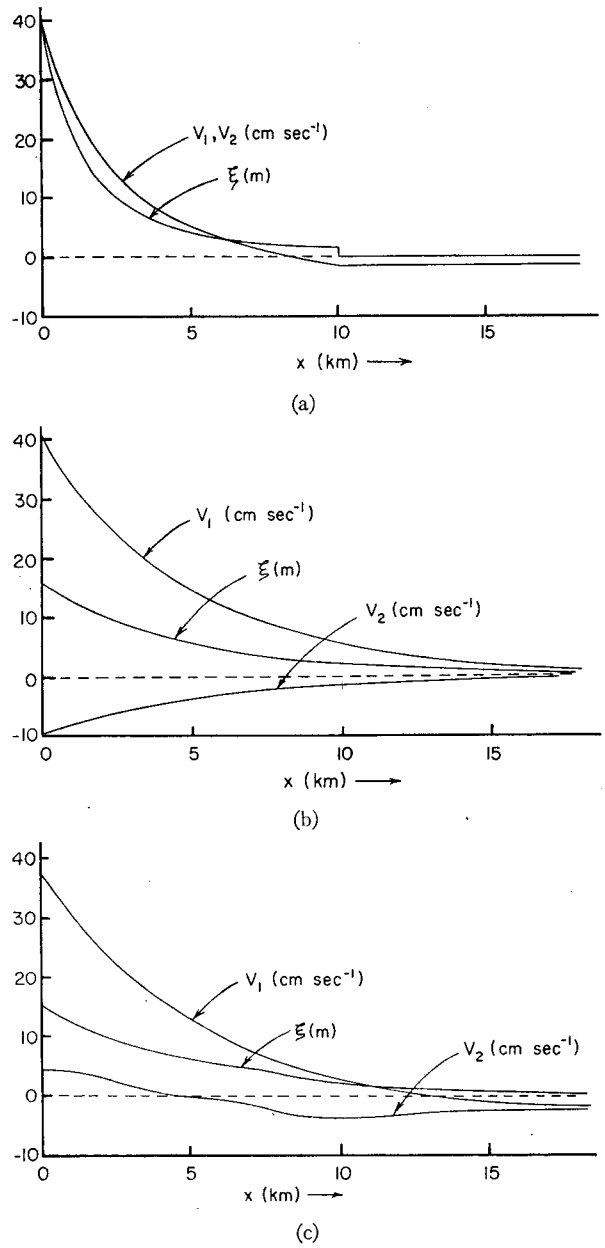

FIG. 2. Average longshore current in upper (V_1) and lower (V_2) layers, and thermocline displacement in the quasi-static response at $t=10^5$ sec for (a) $\Delta\rho=0$, (b) a flat bottom lake, and (c) the case of both topography and stratification.

maximum thermocline displacement is about 40 m, or about twice the depth of the water at the shore, implying that the linearization is not valid. The discontinuity in ξ at $x=10$ km has no physical relevance; it disappears if $h_2(x)$ is differentiable there. On the opposite side of the lake the current would be in the same direction, but the thermocline displacement would be of the opposite sign. If the depth at the shore is allowed to decrease to zero, the longshore velocity and ξ both become infinite, and this inviscid theory breaks down. The reason is that the acceleration $\tau_0/(\rho_0 h)$ becomes infinite. In real lakes, of course, friction is important near the shore. Thus, the maximum magnitudes predicted by this model may not be realistic.

d. The quasi-static response to a longshore wind: A uniform depth lake with $\Delta\rho\neq 0$

A second case where (2.17)–(2.19) can be solved readily is that of a uniform depth lake (h_2=constant). The solution is

$$\left.\begin{aligned} U_2' &= \frac{\tau_y}{\rho_0 f}\left(\frac{h_2}{h_1+h_2}\right)\left[\frac{\cosh\left(\dfrac{x-L_x/2}{\lambda}\right)}{\cosh(L_x/2\lambda)}-1\right] \\ \xi' &= -\frac{\tau_y}{\rho_0 f\lambda}\left(\frac{h_2}{h_1+h_2}\right)\left[\frac{\sinh\left(\dfrac{x-L_x/2}{\lambda}\right)}{\cosh(L_x/2\lambda)}\right] \end{aligned}\right\}, \quad (2.21)$$

where

$$\lambda=\left[\frac{\dfrac{\Delta\rho}{g}h_1h_2}{f^2(h_1+h_2)}\right]^{\frac{1}{2}}$$

is the internal Rossby radius of deformation. For $\Delta\rho/\rho_0=1.25\times10^{-3}$, $h_1=20$ m, $h_2=80$ m (values typical of Lake Ontario in late summer), and the same wind stress as for the previous case (Fig. 2a) the solution is plotted in Fig. 2b. For this case there is also a thin coastal current but of a pure baroclinic nature; the current averaged over depth is zero. (The fact that the average current is zero was shown in Section 2b.) The maximum thermocline displacement is about 16 m, less than half that of the previous case. This solution is the "baroclinic coastal jet" discussed by Charney (1955) and Csanady (1968a, b).

e. The quasi-static response to a longshore wind: Topography and stratification combined

The case where both topography and stratification are important can be solved numerically. Eqs. (2.17) and (2.18) were discretized by using centered differences. The difference equations and Eq. (2.19) then give a complete set of linear algebraic equations which was solved by the numerical method for tridiagonal matrices in Isaacson and Keller (1966).

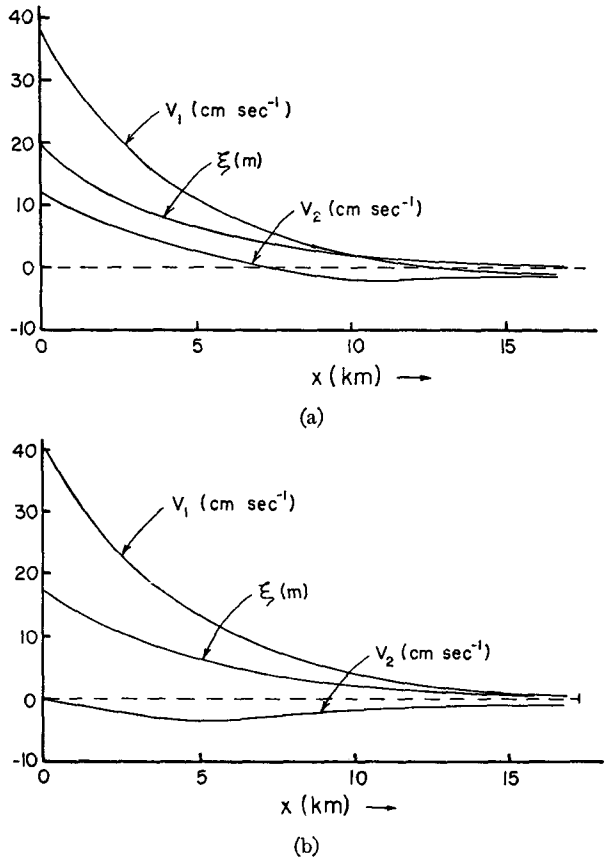

FIG. 3. Average longshore current in upper (V_1) and lower (V_2) layers, and thermocline displacement (ξ) in the quasi-static response at $t=10^5$ sec for two variations on the case of Fig. 2c: (a) half the density difference across the thermocline, and (b) twice the bottom slope.

For $\Delta\rho/\rho_0=1.25\times10^{-3}$, the topography given in Fig. 1, and the same wind stress as above, the solution is shown in Fig. 2c. These values correspond to Lake Ontario in the summer. The major differences between this case and the barotropic case (Fig. 2a) are that the upwelling region is wider, the upper-layer current is larger, and the lower-layer current is smaller.

Two variations on this last case are given in Fig. 3. The first one differs only in that the density difference is half that of Fig. 2c. Consequently, the result is closer to that of the homogeneous case (Fig. 2a). In the second, the density difference is the same as in Fig. 2c but the slope is twice as great (i.e., the slope zone is only half as wide). Thus, the result is similar to that of the constant depth case (Fig. 2b).

f. The response to the onshore-offshore component of the wind

To compute the response to the onshore component of the wind stress, we set $\tau_x=\tau_0$ and $\tau_y=0$. The

analysis for the longshore pressure gradient [Eqs. (2.7) and (2.8)] still holds. Mass continuity still requires that $U_1+U_2=0$ and $\tau_y=0$ implies $g(\partial\xi/\partial y)=0$ [from (2.8)]; thus (2.7) reduces to

$$\frac{\partial}{\partial t}(V_1+V_2)=0.$$

Since $V_1=V_2=0$ at $t=0$, it follows that

$$V_1+V_2=0. \tag{2.23}$$

Using this relation and

$$\left.\begin{aligned} U_1+U_2=0, &\quad \tau_x=\tau_0 \\ g\frac{\partial\eta}{\partial y}=0, &\quad \tau_y=0 \end{aligned}\right\}, \tag{2.24}$$

Eqs. (2.1)–(2.6) can then be reduced to

$$\left(1+\frac{h_1}{h_2}\right)\left(\frac{\partial U_1}{\partial t}-fV_1\right)=\frac{\tau_0}{\rho_0}+g\frac{\Delta\rho}{\rho_0}h_1\frac{\partial\xi}{\partial x}, \tag{2.25}$$

$$\frac{\partial V_1}{\partial t}+fU_1=0, \tag{2.26}$$

$$\frac{\partial\xi}{\partial t}-\frac{\partial U_1}{\partial x}=0. \tag{2.27}$$

The boundary and initial conditions are

$$\left.\begin{aligned} x=0, L_x: &\quad U_1=0 \\ t=0: &\quad U_1=V_1=0, \quad \xi=0 \end{aligned}\right\}. \tag{2.28}$$

The full solution of this problem, for any topography or density difference, is composed of the purely static response given by

$$\left.\begin{aligned} V_1&=-\frac{\tau_0}{\rho_0 f(1+h_1/h_2)} \\ U_1&=0 \\ \xi&=0 \end{aligned}\right\}, \tag{2.29}$$

and an infinite sum of the (oscillatory) free modes of (2.25)–(2.27) which cancels the static response at $t=0$. The static component is analogous to the setup to the longshore component of the wind. The magnitudes of the oscillatory and static components are clearly the same since they cancel at $t=0$ and do not change in magnitude with time.

3. A numerical model

a. The general model

The simple model discussed in Section 2 has two major weaknesses. First, the linearization may not be valid since for realistic winds the thermocline displacements are large. Second, it does not allow for friction in the shallow water. In this section these defects are evaluated by studying a numerical model.

As the linear model did, the numerical model employs the hydrostatic, Boussinesq and rigid lid approximations, and neglects longshore variation. It does, however, allow for detailed vertical structure, nonlinear effects and friction.

For this model, in addition to the symbols in Section 2, it is necessary to define the following:

$w(x,z,t)$	vertical velocity
$T(x,z,t)$	temperature (°C)
$h(x)$	total depth
$p(x,y,z,t)$	deviation of the pressure from a motionless, isothermal (4C) state
$A_z(z,t)$	vertical eddy viscosity
K_z	vertical eddy diffusivity of heat (1.0 cm^2 sec^{-1})
A_x	horizontal eddy viscosity and eddy diffusivity (10^4 cm^2 sec^{-1})
$\rho'(x,z,t)$	deviation of the density from that at 4C
ρ_0	density at 4C (1.000 gm cm^{-3})
$\tau_{zx}(x,z,t)$	x component of vertical shear stress
$\tau_{zy}(x,z,t)$	y component of vertical shear stress
Δx	horizontal grid separation (6.33 km)
Δz	vertical grid separation (6.67 m)
Δt	time step (1250 sec)

The equations of the model are as follows:

$$\frac{\partial u}{\partial t}=-\frac{\partial}{\partial x}(uu)-\frac{\partial}{\partial z}(wu)+fv-\frac{1}{\rho_0}\frac{\partial p}{\partial x}+\frac{1}{\rho_0}\frac{\partial\tau_{zx}}{\partial z}+A_x\frac{\partial^2 u}{\partial x^2} \tag{3.1}$$

$$\frac{\partial v}{\partial t}=-\frac{\partial}{\partial x}(uv)-\frac{\partial}{\partial z}(wv)-fu-\frac{1}{\rho_0}\frac{\partial p}{\partial y}+\frac{1}{\rho_0}\frac{\partial\tau_{zy}}{\partial z}+A_x\frac{\partial^2 v}{\partial x^2} \tag{3.2}$$

$$\frac{\partial T}{\partial t}=-\frac{\partial}{\partial x}(uT)-\frac{\partial}{\partial z}(wT)+K_z\frac{\partial^2 T}{\partial z^2}+A_x\frac{\partial^2 T}{\partial x^2} \tag{3.3}$$

$$0=-\frac{1}{\rho_0}\frac{\partial p}{\partial z}-\frac{\rho'}{\rho_0}g \tag{3.4}$$

$$\frac{\partial u}{\partial x}+\frac{\partial w}{\partial z}=0 \tag{3.5}$$

$$\frac{\rho'}{\rho_0}=-6.8\times10^{-6}(T-4)^2. \tag{3.6}$$

The first two are momentum equations for the onshore (x direction) and longshore (y direction) com-

ponents of velocity. The others are the thermodynamic energy equation, the hydrostatic equation, the incompressibility condition, and the approximate nonlinear equation of state for fresh water developed by Simons (1971b).

At the bottom a no-slip condition is imposed: $u=v=w=0$. At the surface the vertical motion is set to zero (the rigid lid approximation) and the stress is specified. Since the experiments were only run for 2–3 days, the surface heat flux was set equal to zero as well as the bottom heat flux.

The pressure gradient terms in (3.1) and)(3.2 are computed diagnostically from the hydrostatic equation and mass balance constraints. As in Section 2, $\partial\rho/\partial y$ is a function only of time chosen so that the total flow normal to the cross section is zero.

The vertical shear stress was computed in the interior of the fluid from

$$\left.\begin{aligned}\tau_{zx}&=\rho_0 A_z(z,t)\frac{\partial u}{\partial z}\\ \tau_{zy}&=\rho_0 A_z(z,t)\frac{\partial v}{\partial z}\end{aligned}\right\}, \tag{3.7}$$

where $A_z(z,t)$ can be prescribed as a function of depth and time; the actual values used here are given in Section 3b. At the bottom boundary, the shear stress was computed from

$$\left.\begin{aligned}\tau_{zx}&=\rho_0 0.002(u_0^2+v_0^2)^{\frac{1}{2}}u_0\\ \tau_{zy}&=\rho_0 0.002(u_0^2+v_0^2)^{\frac{1}{2}}v_0\end{aligned}\right\}, \tag{3.8}$$

where u_0 and v_0 are the velocity components at the first grid level above the bottom. The value of the drag coefficient (0.002) is a commonly quoted "typical" value for turbulent flow. A better estimate would require a knowledge of the bottom roughness. The two formulas for computing the shear stress give roughly the same bottom stress for the cases studied below.

The numerical scheme used here is essentially the same as that used by Bryan and Cox (1968). It uses the "leap frog" centered time difference scheme for all terms but the diffusion terms which are forward differenced in time. The spatial derivatives are also evaluated by centered differences. This scheme used with the flux form of the equations gives conservation of mass, momentum and energy. The value of Δz (6.67 m) was chosen so that the surface Ekman layer was adequately resolved. The value of Δx was chosen by making $\Delta z/\Delta x$ equal to the bottom slope; this gives essentially the same horizontal resolution as vertical resolution in the main region of interest and simplifies the computation. The time step was chosen as the largest consistent with computational stability; the classical stability criterion for the vertical diffusion terms, $\Delta t \leqslant \Delta z^2/2A_z$, gives a good estimate since it gives a smaller time step than the criterion for pure advection or internal wave propagation.

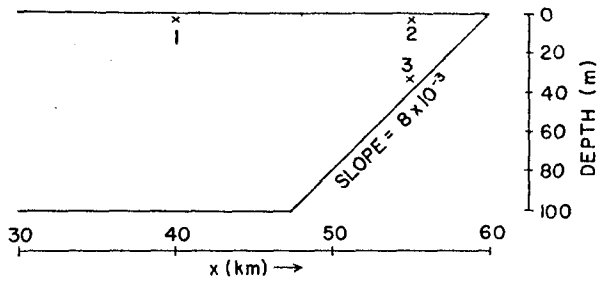

FIG. 4. Idealized cross section used in the numerical model. The numbered points are referred to in the text.

b. Numerical values of the parameters for Lake Ontario

1) The bottom topography (Fig. 4) consists of a linear slope region from zero depth at the shore to a depth of 100 m at 12.5 km from the coast. The central region has a depth of 100 m and a width of 35 km. The total width of the lake is 60 km. This cross-section shape is similar to that of Lake Ontario.

2) The initial condition is a state of rest. A wind stress of magnitude 1.0 dyn cm^{-2} is then applied and allowed to last for 1.0×10^5 sec, at which time it returns to zero.

3) While the wind lasts the vertical eddy viscosity $A_z(z)$ is 100 cm^2 sec^{-1} at the surface and falls off exponentially to 10 cm^2 sec^{-1} at depth of 100 m. After the wind stress drops to zero, the eddy viscosity is set equal to 10 cm^2 sec^{-1} at all depths.

4) The horizontal eddy viscosity and diffusivity A_x was chosen to be 10^4 cm^2 sec^{-1}. This value is larger than any reported by Csanady (1963) and Murthy

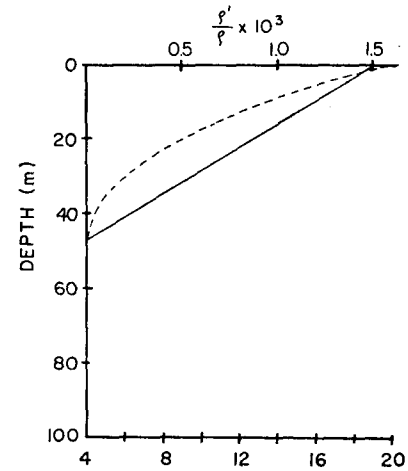

FIG. 5. Initial temperature distribution used in the stratified numerical experiment (solid line), and the corresponding density distribution (dashed line).

(1972), but the numerical solutions given below were found to be very insensitive to the value of A_z in the range 10^3–10^5 cm^2 sec^{-1}. The reason is that the vertical friction force in (3.1) and (3.2) is larger than the horizontal friction force in both the interior and coastal regions.

Results will be presented for the three cases defined as follows:

CASE A: The wind is in the longshore (positive y) direction and the lake is homogeneous.

CASE B: The wind is in the longshore direction and the lake is stratified.

For the stratified case it was necessary to experiment a little before choosing the initial temperature distribution and the vertical diffusivity K_z. When the initial temperature structure contained a sharp thermocline, spatial truncation error was large; with the centered difference scheme for advection, this led to unstable stratification and thus thermal convection. On the other hand, increasing the vertical thermal diffusivity remedied this but destroyed the thermocline. The lesson, of course, is that the temperature field must be adequately resolved. To balance computational ease with physical reality, it was decided to use as the initial condition the temperature field shown in Fig. 5. The corresponding density field, also shown in Fig. 5, corresponds roughly to the case of Section 2 where the thermocline was 20 m deep and the density jump across it was 1.25×10^{-3}.

The influence of wind mixing on the time evolution of this temperature field can be estimated from the

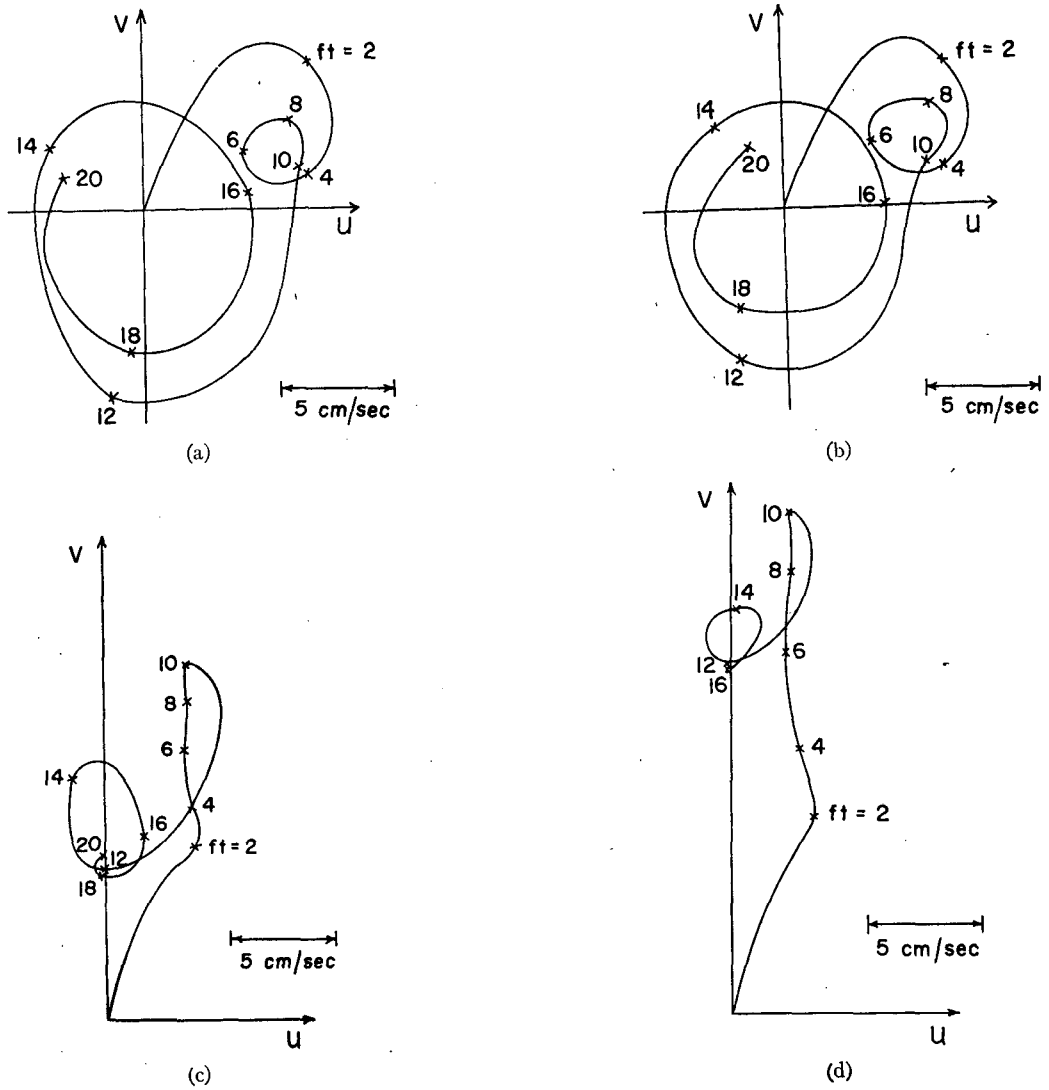

FIG. 6. Surface hodographs for a longshore wind stress of 1 dyn cm^{-2}: (a) station 1 of Fig. 4 (20 km from shore) for a homogeneous lake, (b) station 1 for a stratified lake, (c) station 2 of Fig. 4 (5 km from shore) for a homogeneous lake, and (d) station 2 for a stratified lake.

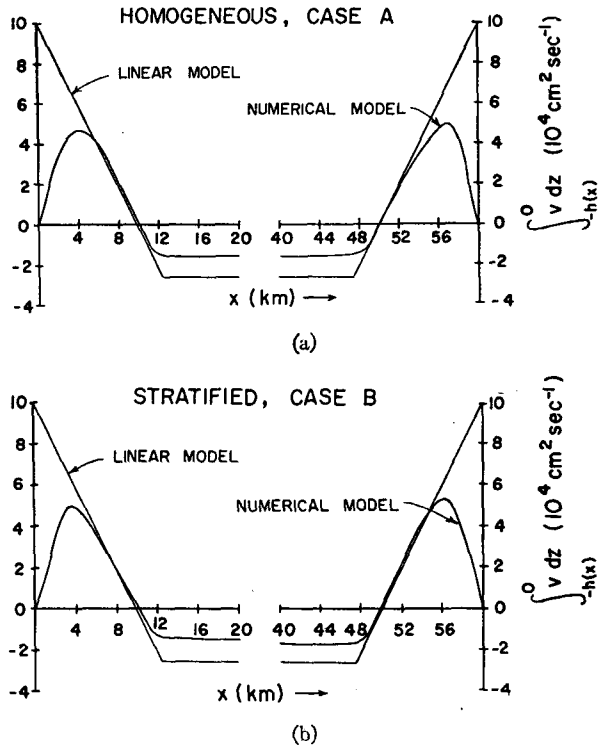

FIG. 7. Longshore transport at $t=10^5$ sec for a homogeneous lake (a) and a stratified lake (b).

experimental results of Kato and Phillips (1969). They predict that the wind will cause a mixed layer whose depth D varies with time according to

$$D(t)=u_*\left(\frac{15t}{N_0^2}\right)^{\frac{1}{2}}. \tag{3.9}$$

For $t=10^5$ sec, $u_*=(\tau_0/\rho_0)^{1/2}=1$ cm sec^{-1}, N_0 (the buoyancy frequency)$=2.7\times10^{-2}$ sec^{-1}, and the depth of the homogeneous layer is about 12.5 m. Since this amounts to a temperature variation of about 2C, which is independent of x, it will have little effect on the currents. It was therefore decided to essentially ignore vertical mixing of heat, retaining only a small amount to smooth the numerical solution slightly. The value of K_z used for smoothing was 1.0 cm^2 sec^{-1}.

c. Surface hodographs

As the first step in analyzing the two cases, time-dependent surface hodographs for two points will be shown for each. One point is in the interior of the lake, 20 km from shore (no. 1 in Fig. 4), and the second is in the shore zone, 5 km from shore (no. 2 in Fig. 4).

Since in the interior region the flow is almost horizontally uniform, the hodographs shown are representative of the entire region. For the homogeneous case (Fig. 6a) and the stratified case (Fig. 6b), the response to the longshore component of the wind is nearly the same. While the wind lasts the current is approximately the surface current of the classical Ekman spiral plus a decaying inertial oscillation. After the wind stress drops to zero ($t=10^5$ sec, $ft=10$) the current is an inertial oscillation which decays more slowly since the viscosity is less. The response to the onshore component of the wind is similar but rotated 90° to the right.

The response in the interior is what one would expect from the solution of Fredholm [given in Ekman (1905)] for the inertial oscillation in an infinite sea of constant eddy viscosity. The small differences are due to the pressure gradient acceleration, the variable eddy viscosity and truncation error. To provide a better model for the interior current, one might assume the region is horizontally uniform and attempt to model the vertical structure by using greater vertical resolution and parameterizing the turbulent transport of momentum better.

Fig. 6c shows the surface current in the shore zone for a longshore wind and no stratification (Case A). While the wind lasts, the current is approximately in the wind direction and increases with time. After the wind stress drops to zero ($t=10^5$ sec), there is an inertial oscillation superimposed over a decay of the geostrophic component. The same general pattern holds for the stratified case (Fig. 6d), but the current is larger and does not decay as fast. This can be understood by using the results of the linear model of Section 2. There it was shown that the effect of

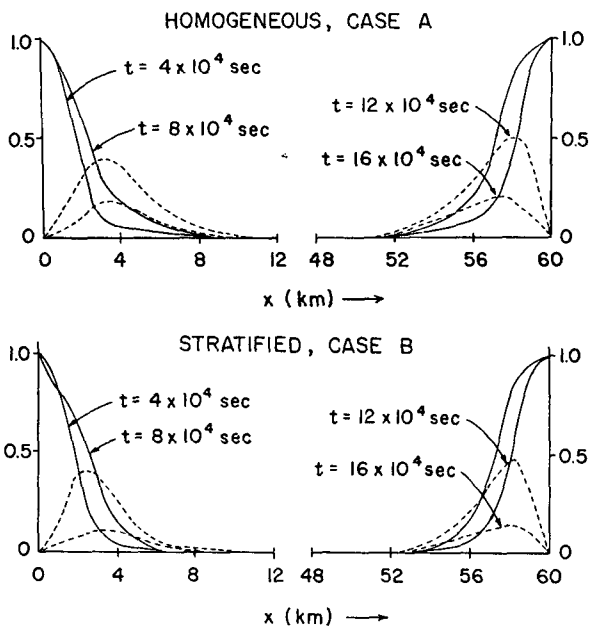

FIG. 8. Longshore component of bottom stress (dyn cm^{-2}) for a homogeneous lake (a) and a stratified lake (b). The solid lines are for times when the wind stress is 1 dyn cm^{-2} and the dashed lines are for the decay period when the wind stress is zero.

stratification was to increase the surface current and to decrease the bottom current. Since the bottom current is smaller, the decay through bottom friction is slower. This result is similar to that of Holton (1965).

In contrast to this response to the longshore component of the wind, the current near the shore for the onshore component of the wind is smaller than in the interior. This is consistent with the results of Section 2.

d. The vertically integrated flow for a longshore wind

To further analyze the response of the model lake to a longshore wind, we now consider the vertically integrated flow. If the small horizontal friction terms are neglected, Eq. (3.2) can be integrated to give

$$\frac{\partial}{\partial t}\int_{-h(x)}^{0} v\,dz=-\frac{\partial}{\partial x}\int_{-h(x)}^{0} uv\,dz-\frac{h(x)}{\rho_0}\frac{\partial p}{\partial y}+\frac{\tau_{zy}(z=0)-\tau_{zy}(z=-h(x))}{\rho_0}, \quad (3.10)$$

where the fact that

$$\int_{-h(x)}^{0} u\,dz=0$$

has been used. As in the model of Section 2, the longshore pressure gradient $\partial p/\partial y$ is independent of x and z and is determined from the imposed condition

$$\int_{-h(x)}^{0}\int_{0}^{L_x} v\,dx\,dz=0.$$

This equation shows that the only factors which change the vertically integrated longshore flow are the longshore pressure gradient (which is barotropic), advection of momentum by the onshore-offshore component, and the top and bottom stresses. As in Section 2, neither the density perturbation nor the Coriolis parameter appears explicitly.

The longshore transport at $t=10^5$ sec is given in Fig. 7a for the homogeneous case and in Fig. 7b for the stratified case, along with the prediction of the linear frictionless theory of Section 2. In general, the numerical model gives a weaker flow in both the shore zone and the interior. In the shore zone, this can be explained by the loss of momentum through the bottom. The longshore component of the bottom stress [computed from Eq. (3.8)] is given in Fig. 8a for the homogeneous case and in Fig. 8b for the stratified case. While the wind lasts, the stress near the shore is nearly equal to the surface stress but is neg-

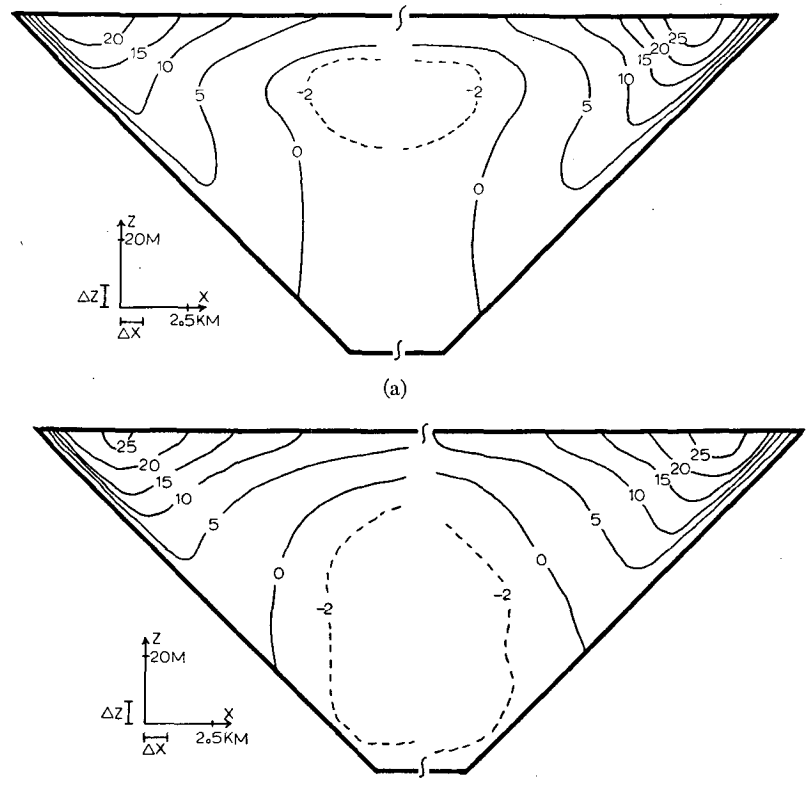

FIG. 9. Longshore current V (cm sec^{-1}) at $t=10^5$ sec for a homogeneous lake (a) and a stratified lake (b). The uniform central region of width 30 km is not shown.

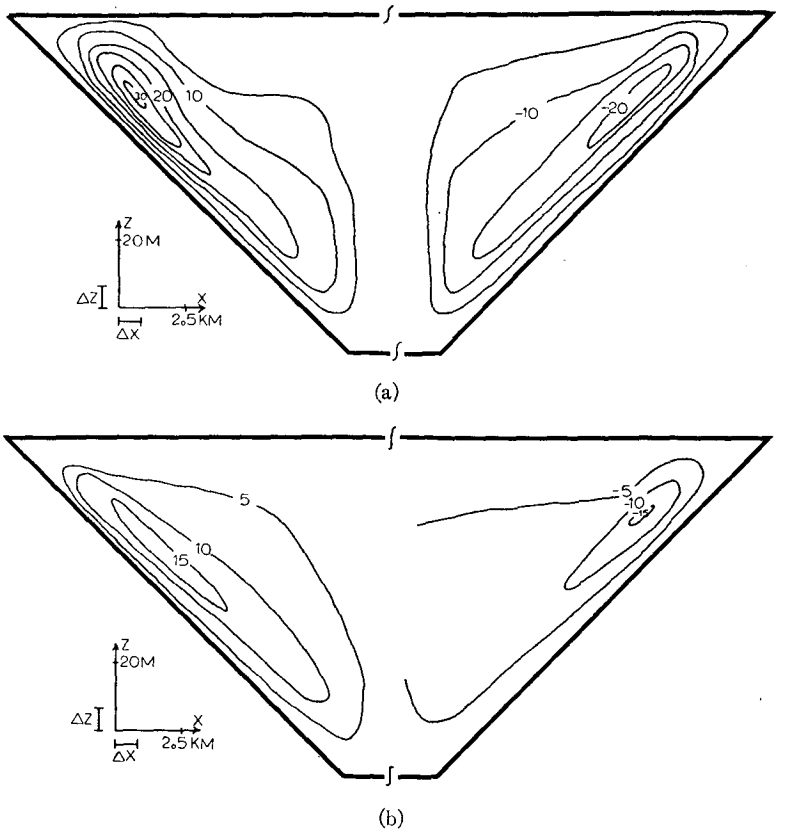

FIG. 10. Vertical motion (10^{-3} cm sec^{-1}) at $t=10^5$ sec for a homogeneous lake (a) and a stratified lake (b).

ligible at 4 km or more from the shore. After the wind stops ($t=10^5$ sec), the bottom stress has a maximum offshore since the shallow water is quickly decelerated. The weaker flow in the interior is due to the smaller longshore pressure gradient rather than to local bottom friction; the computed longshore pressure gradient is about 15% less than that given by the "setup" relation [Eq. (2.8)]. This result can be contrasted with the case of a uniform depth sea where bottom friction increases the longshore pressure gradient (Ekman, 1905). For the case of no rotation and constant eddy viscosity the increase is 50%.

The asymmetry between the two sides of the lake in Figs. 7 and 8 is due to advection of momentum. Since

$$\int_{-h(x)}^{0} uvdz$$

is positive, the momentum is advected to the right. However, at the same shore momentum is advected downward, accelerating the bottom flow and increasing the bottom stress. Thus, horizontal advection of momentum tends to be compensated by increased bottom drag.

e. The longshore current field for a longshore wind

The full x-z distribution of the longshore current at $t=10^5$ sec is given in Fig. 9a for the homogeneous case and in Fig. 9b for the stratified case. As in the theory of Section 2, the width of the coastal current is smaller for the homogeneous case, but it extends to a greater depth. At no point does the current differ by more than 5 cm sec^{-1} between the two cases. However, the current shear (surface current minus the current just above the bottom) differs by as much as 8 cm sec^{-1}; this is consistent with the thermal wind equation.

f. Vertical motion for a longshore wind

To analyze the vertical motion, first the spatial variation for $t=10^5$ sec will be shown. Next the time variation at two points where the vertical motion is large will be presented.

Fig. 10a shows the x-z distribution of w for the homogeneous case at 10^5 sec; Fig. 10b gives the same for the stratified case. As predicted by the linear theory of Section 2, the vertical motion is larger but confined to a thinner region near the coast for the homogeneous case. However, the maximum vertical

motion is less in the numerical model and occurs about 3 km offshore. The numerical results also show a larger vertical velocity on the upwelling side than on the downwelling side. This is not true for all times, as can be seen in Fig. 11. These figures show the vertical velocity versus time at a depth of about 35 m and 5 km from shore (point 3 in Fig. 4) and at the corresponding point on the opposite side. The two curves would be mirror images of each other in linear theory. The fact that they are not is probably due to the interaction of the inertial oscillation with the geostrophic current. This interaction is important when the relative vorticity is comparable to the Coriolis parameter (Magaard, 1968), as is the case here.

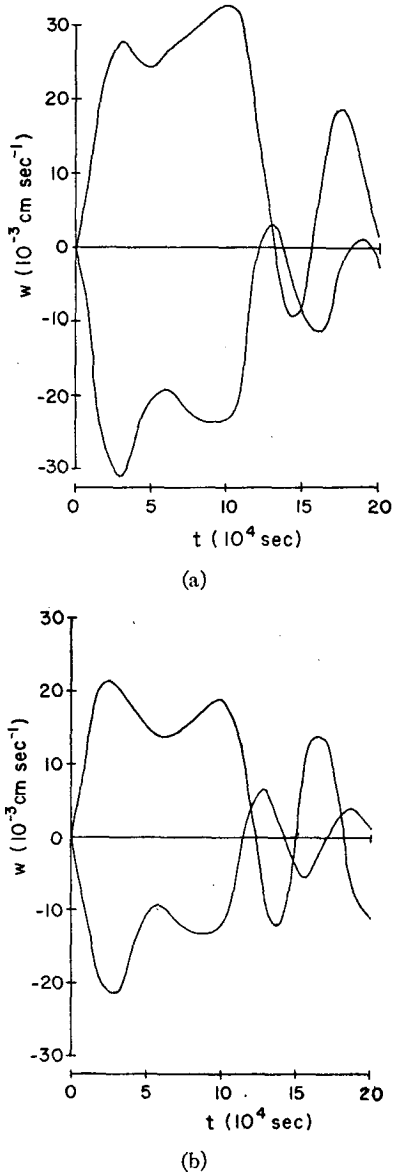

FIG. 11. Vertical motion (10^{-3} cm sec^{-1}) at Station 3 of Fig. 4 for a homogeneous lake (a) and a stratified lake (b).

g. The temperature field for a longshore wind

Since vertical diffusion is small, vertical displacements can be estimated from the temperature field. Fig. 12 gives temperature versus time at point 3 in Fig. 4 and at the corresponding point on the opposite side for the stratified case. While the wind lasts, the temperature changes by about 3.5C; the vertical displacement is about 10 m. In the inertial oscillation which follows, the displacement is about 1 m.

The full x-z temperature distribution at $t=10^5$ sec is shown in Fig. 13. Although the greatest vertical motion has occurred in the shore zone, there is approximately a 1.5C drop in temperature across the interior region also.

4. Summary and concluding remarks

In the Introduction the following questions were posed:

1. What general pattern of large-scale currents would be generated if a storm passed over a lake?
2. What is the relative importance of topography, rotation, friction, inertial accelerations and stratification in determining the currents?

By combining the model results presented here with previous theories and with observational evidence from Lake Ontario, it is now possible to develop a coherent answer to these questions. It is natural to begin with the vertically integrated flow.

In both the linear model of Section 2 and the numerical model of Section 3 the vertically integrated flow follows the same pattern; the water in the shallow regions is accelerated in the direction of the longshore component of the wind and the flow is returned in the deeper central region of the lake. In the linear model this result was shown to be independent of both stratification and rotation; in the numerical model it was shown that friction does not affect this

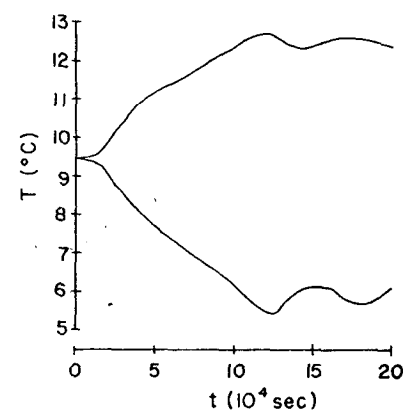

FIG. 12. Temperature vs time at Station 3 of Fig. 4 (top curve) and the corresponding point on the opposite side of the lake (bottom).

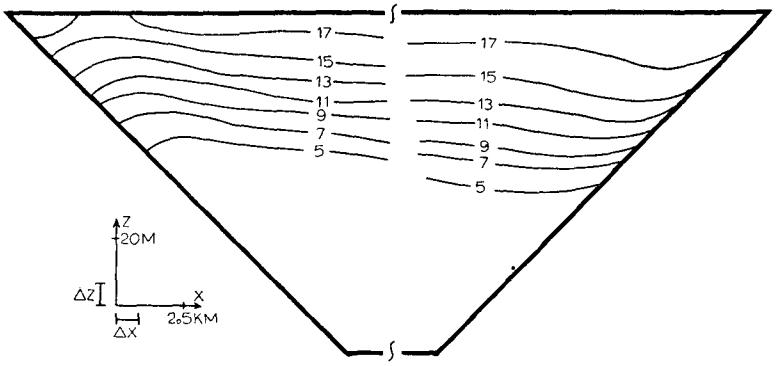

FIG. 13. Temperature field after a longshore wind of 1 dyn cm^{-2} has been blowing for 10^5 sec. The initial temperature field is given in Fig. 5.

pattern but decreases the magnitude of the flow. This flow pattern is the closed basin analogy to what Weenink and Groen (1958) call the "bottom slope current" since it is due to a constant wind stress acting on a basin of variable depth. This result is clearly consistent with the numerical results of Simons (1972) and Rao and Murty (1970). Thus, in some sense, this result can be regarded as being "well known." However, these numerical models do not provide simple formulas, such as Eq. (2.19), which can be readily checked against observations; nor do they provide the physical insight which an analytic theory does.

Csanady (1973) has shown that this equation is essentially correct for an episode in Lake Ontario where the wind changed rapidly. Another example from Csanady's coastal chain observations, when the wind was relatively steady, has been cited by Birchfield (1973) as a case where his steady-state theory is more applicable. His theory also gives a two-cell flow pattern, but the cells are rotated 90° counterclockwise from those in the present theory, i.e., the strongest coastal currents are to the left of the wind at the upwind and downwind shores. However, since the currents are clearly not steady in Birchfield's example (the average longshore transport nearly doubles in a little over a day), the transient theory presented here may be more applicable. It is difficult to decide between the two with information at only one section of shoreline.

It is interesting to note that the lowest second-class (rotational) mode of an elliptic paraboloid (Ball, 1965) consists of a two-cell pattern also, but the two cells rotate counterclockwise. If one models Lake Ontario as an elliptic paraboloid three times as long as it is wide, this mode would have a period of approximately eight days. Thus, the two-cell pattern predicted here can be expected to rotate slowly counterclockwise as it decays; or, if the wind remains constant for a sufficient period, the cells could rotate into the steady pattern predicted by Birchfield.

Both models also give similar results for the component of velocity normal to the shore and the vertical motion. In the surface layer the normal component is dominated by Ekman drift and the inertial oscillation. At greater depths, in addition to the inertial oscillation, there is a flow to the left of the wind. There, the Coriolis force due to this component is balanced by the longshore pressure gradient and the time derivative of the longshore component. As could be expected, there is upwelling to the left of the wind and downwelling to the right. The magnitude of the vertical motion depends on the bottom slope and stratification; both stratification and gentle slopes tend to decrease the maximum value and thus widen the coastal boundary layer.

Whereas the vertically averaged longshore flow is not very sensitive to friction and stratification, the vertical distribution of the current is. By suppressing vertical motion, stratification confines most of the effect of the wind to the epilimnion. Because of the vertical shear (thermal wind) across the thermocline, the effect of bottom friction in causing the current to decay is decreased also. Thus, one can explain Csanady's (1972c) observation that the maximum current increases from spring to summer by the effect of stratification in causing larger surface currents to be generated or by its slowing their decay.

In general, nonlinear effects were found to be relatively minor. Advection of longshore momentum into the shore zone can be important, but it tends to be compensated by bottom friction. The phase of the inertial oscillation was shown to be sensitive to nonlinear effects but its amplitude was roughly unchanged. The importance of the inertial terms may be much greater in three-dimensional models since there would be advection by the larger longshore component of velocity.

Our experience with currents in the atmosphere and ocean teaches us to be skeptical of two-dimensional models. It is well known, for example, that even the zonally averaged circulation of the atmosphere depends strongly on interactions with nonsymmetric disturbances. These disturbances can arise from differential heating, topography, or through instabilities of the

zonal flow. Nevertheless, it is likely that the two-dimensional theory presented here can explain not only the magnitude of wind-driven flow but many of the qualitative features of it.

Acknowledgments. I thank Profs. Theodore Green, Heinz Lettau and John Young of the University of Wisconsin and Prof. G. T. Csanady of the University of Waterloo for reading earlier drafts of this work. Financial support was supplied by the National Science Foundation, under Grant No. GA-33140, and by Argonne National Laboratory, under a predoctoral fellowship.

REFERENCES

Ball, F. K., 1965: Second-class motions of a shallow liquid. *J. Fluid Mech.*, **23**, 545–561.

Bennett, J. R., 1972: A theory of large-amplitude Kelvin waves. *J. Phys. Oceanogr.*, **3**, 57–60.

Birchfield, G. E., 1967a: Horizontal transport in a rotating basin of parabolic depth profile. *J. Geophys. Res.*, **72**, 6155–6163.

——, 1967b: Wind-driven currents in a long rotating channel. *Tellus*, **19**, 243–249.

——, 1969: The response of a circular model Great Lake to a suddenly imposed wind stress. *J. Geophys. Res.*, **74**, 5547–5554.

——, 1972: Theoretical aspects of wind-driven currents in sea or lake of variable depth with no horizontal mixing. *J. Phys. Oceanogr.*, **2**, 355–366.

——, 1973: An Ekman model of coastal currents in a lake or shallow sea. *J. Phys. Oceanogr.*, **3**, 419–428.

Bryan, Kirk, and M. D. Cox, 1968: A nonlinear model of an ocean driven by wind and differential heating. Part 1: Description of the three-dimensional velocity and density fields. *J. Atmos. Sci.*, **25**, 945–967.

Charney, J. G., 1955: Generation of oceanic currents by wind. *J. Marine Res.*, **14**, 477–498.

Csanady, G. T., 1963: Turbulent diffusion in Lake Huron. *J. Fluid Mech.*, **17**, 360–384.

——, 1967: Large-scale motion in the Great Lakes. *J. Geophys. Res.*, **72**, 4151–4162.

——, 1968a: Wind-driven summer circulation in the Great Lakes. *J. Geophys. Res.*, **73**, 2579–2589.

——, 1968b: Motions in a model Great Lake due to a suddenly imposed wind. *J. Geophys. Res.*, **73**, 6435–6447.

——, 1972a: Response of large stratified lakes to wind. *J. Phys. Oceanogr.*, **2**, 3–13.

——, 1972b: The coastal boundary layer in Lake Ontario. Part I: The spring regime. *J. Phys. Oceanogr.*, **2**, 41–53.

——, 1972c: The coastal boundary layer in Lake Ontario: Part II: The summer-fall regime. *J. Phys. Oceanogr.*, **2**, 168–176.

——, 1973: Wind-induced barotropic motions in long lakes. *J. Phys. Oceanogr.*, **3**, 429–438.

——, and B. Pade, 1972: Coastal Jet Project. 1971 Annual Report, Environmental Fluid Mech. Lab., University of Waterloo.

Ekman, V. W., 1905: On the influence of the earth's rotation on ocean currents. *Ark. Mat. Astron. Fys.*, **2**, 1–53.

Hess, S. L., 1959: *Introduction to Theoretical Meteorology*. New York, Holt, Rinehart and Winston, 362 pp.

Holton, J. R., 1965: The influence of viscous boundary layers on transient motions in a rotating stratified fluid: Part. II. *J. Atmos. Sci.*, **22**, 535–540.

Hurlburt, H. E., and J. D. Thompson, 1972: Coastal upwelling on a β-plane. *J. Phys. Oceanogr.*, **3**, 16–32.

Isaacson, E., and H. B. Keller, 1966: *Analysis of Numerical Methods*. New York, Wiley, 541 pp.

Kato, H., and O. M. Phillips, 1969: On the penetration of a turbulent layer into a stratified fluid. *J. Fluid Mech.*, **37**, 643–655.

Killworth, P. D., 1973: A two-dimensional model for the formation of Antarctic Bottom Water. *Deep-Sea Res.*, **20**, 941–971.

Landsberg, D. R., J. T. Scott and M. Fenlon, 1970: Summer circulation patterns near Nine Mile Point, Lake Ontario. *Proc. 13th Conf. Great Lakes Res.*, Intern. Assoc. Great Lakes Res., 444–452.

Lick, Wilbert, 1972: The time-dependent flow in an infinitely long lake. *Abstracts 15 Conf. Great Lakes Res.*, Intern. Assoc. Great Lakes Res., 106.

Magaard, L., 1968: Ein Beitrag zur Theorie der internen Wellen als storungen geostrophischer Stromungen. *Deut. Hydrogr. Z.*, **21**, 242–278.

Murthy, C. R., 1972: Complex diffusion processes in coastal currents of a lake. *J. Phys. Oceanogr.*, **2**, 80–90.

O'Brien, J. J., and H. E. Hurlburt, 1972: A numerical model of coastal upwelling. *J. Phys. Oceanogr.*, **2**, 14–26.

Paskausky, D. F., 1971: Winter circulation in Lake Ontario. *Proc. 14th Conf. Great Lakes Res.*, Intern. Assoc. Great Lakes Res., 593–606.

Phillips, O. M., 1966: *The Dynamics of the Upper Ocean*. Cambridge University Press, 261 pp.

Platzman, G. W., 1963: The dynamical prediction of wind tides on Lake Erie. *Meteor. Monogr.*, 4, No. 26, 44 pp.

Rao, D. B., 1967: Response of a lake to a time-dependent wind stress. *J. Geophys. Res.*, **72**, 1697–1708.

——, and T. S. Murty, 1970: Calculation of the steady state wind-driven circulations in Lake Ontario. *Arch. Meteor. Geophys. Bioklim.*, **A19**, 195–210.

Rossby, C. G., 1938: On the mutual adjustment of pressure and velocity distributions in certain simple systems, II. *J. Marine Res.*, **1**, 239–263.

Scott, J. T., P. Jekel and M. W. Fenlon, 1971: Transport in the baroclinic coastal current near the south shore of Lake Ontario in early summer. *Proc. 14th Conf. Great Lakes Res.*, Intern. Assoc. Great Lakes Res., 640–653.

——, and D. Landsberg, 1969: July currents near the south shore of Lake Ontario. *Proc. 12th Conf. Great Lakes Res.*, Intern. Assoc. Great Lakes Res., 705–722.

——, and L. Lansing, 1967: Gradient circulation in Eastern Lake Ontario, *Proc. 10th Conf. Great Lakes Res.*, Great Lakes Res. Div., The University of Michigan, 322–336.

Simons, T. J., 1971a: Development of numerical models of Lake Ontario. *Proc. 14 Conf. Great Lakes Res.*, Intern. Assoc. Great Lakes Res., 654–669.

——, 1971b: Development of three-dimensional numerical models of the Great Lakes. Tech. Report from the Canadian Centre for Inland Waters, Burlington, Ontario.

——, 1972: Development of numerical models of Lake Ontario, Part II. Paper presented at 15th Conf. Great Lakes Res., Madison, Wisc., 5–7 April.

Walin, G., 1972: On the hydrographic response to transient meteorological disturbances. *Tellus* **24**, 169–186.

Weenink, M. P., and P. Groen, 1958: A semi-theoretical, semi-empirical approach to the problem of finding wind effects on water levels in a shallow partly-enclosed sea. *Koninkl. Ned. Akad. Wetenschap. Proc.*, **B61**, 198–213. (Summarized on p. 632 of Groen, P. and G. W. Groves, 1962: Surges. *The Sea*, Vol. 1, M. N. Hill, Ed. New York, Interscience.)